J. Chem. Sci. Vol. 129, No. 11, November 2017, pp. 1781–1786.
https://doi.org/10.1007/s12039-017-1396-x

REGULAR ARTICLE

Special Issue on Recent Trends in the Design and Development of Catalysts and their Applications

Syngas production from the CO_2 reforming of methane over $Co/Mg_{1-x}Ni_xO$ catalysts

FARIS A J AL-DOGHACHI[a] and YUN HIN TAUFIQ-YAP[b,*]
[a]Department of Chemistry, Faculty of Science, University of Basrah, Basrah, Iraq
[b]Department of Chemistry, Faculty of Science, University Putra Malaysia, 43400 UPM Serdang, Selangor, Malaysia
E-mail: taufiq@upm.edu.my

MS received 24 May 2017; revised 28 June 2017; accepted 17 July 2017; published online 11 November 2017

Abstract. By using catalysts of $Co/Mg_{1-x}Ni_xO$ (x= 0, 0.03, 0.07, 0.15; 1 wt% Co each), we performed the dry reforming of methane. The catalysts were prepared by K_2CO_3 co-precipitation from aqueous nickel nitrate hexahydrate and magnesium nitrate hexahydrate. Impregnation of cobalt(II)acetylacetonate onto MgO-NiO was then conducted. TEM, XRD, FTIR, XRF, XPS, and BET characterizations of the catalysts were carried out. Results showed that the catalysts were reduced at 700 °C by H_2 prior to each reaction. CH_4 and CO_2 conversions at 900 °C of the catalysts after being tested for 200 h decreased in the arrange $Co/Mg_{0.85}Ni_{0.15}O$, $Co/Mg_{0.93}Ni_{0.07}O$, $Co/Mg_{0.97}Ni_{0.03}O$, and Co/MgO. The highest H_2 and CO selectivities were observed at a 1:1 CH_4:CO_2 mole ratio. We further performed a dry reforming in the presence of low-concentration oxygen flow (1.25 Vol %) and found an increased CH_4 conversion.

Keywords. Synthesis gas; H_2 production; dry-reforming of biogas; MgO-NiO catalyst.

1. Introduction

In Indonesia and Malaysia, biomass from palm oil has considerable potential for sustainable production of chemicals and fuels because of its renewability and copiousness. However, palm-oil mill effluents (POME) originating from palm-oil mills are a known wastewater pollutant. POME is mainly treated by anaerobic digestion in the palm-oil industry to reach the water-quality standards for industrial effluent. However, one of the byproducts of this process is biogas primarily contains two greenhouse gases [*i.e.*, 60–70% methane (CH_4), 30–40% CO_2, and trace amounts of hydrogen sulfide (H_2S)][1,2] In a method called the dry reforming of methane (DRM), CH_4 and CO_2 produce the highly costly syngas (containing CO and H_2) as feedstock. Accordingly, DRM is eliciting considerable interest because of its environmental benefits.

Researchers have proposed the reformation of methane catalytically with CO_2. The method for the reformation of methane is the dry reforming method (DRM) (Eq. 1).[3]

$$CH_4 + CO_2 \rightarrow 2CO + 2H_2 \quad \Delta H^\circ_{298K} = 247 kJ/mol \tag{1}$$

However, several drawbacks are observed in the DRM reaction. The main drawback is the formation of coke, which occurs when methane gas decomposes (Eq. 2), and the Boudouard reaction (Eq. 3). By contrast, the effects of nickel-based catalysts can reportedly be limited or reduced with the addition of promoters in the deactivation process. Concentrated Lewis bases (e.g., MgO and CaO) that have been improved with the chemisorb of CO_2, have the ability to reduce the deposition of coke when they react with C in the formation of CO. Likewise, lanthanide elements, such as ZrO_2 and La_2O_3, with the ability of storage and release of oxygen exhibit the same effects. During the reaction between carbon deposits and lattice oxygen formed in these redox oxides, carbon is being removed.[4]

$$CH_4 \rightarrow C + 2H_2\Delta \quad H^\circ_{298K} = 75 kJ/mol \tag{2}$$

$$2CO \rightarrow C + CO_2\Delta \quad H^\circ_{298K} = -172 kJ/mol \tag{3}$$

The use of nickel is highly recommended for the reforming process, as this active metal is readily available and is inexpensive. However, the main disadvantage of nickel is that it causes the formation of carbon

---

[*] For correspondence

that brings about catalytic deactivation rather easily.[5] Consequently, research was conducted with the aim of improving the activities of catalysts and the stability of Ni catalysts in the reforming process.[6] When strong Lewis base promoters, such as MgO or CaO were added, the Ni-based catalysts became deactivated. However, this can be improved with the chemisorbing of CO_2, to reduce the deposit of coke that reacts with deposited carbon to form carbon monoxide.[4]

As such, the aim of the research study is to prepare a catalyst with high selectivity, activity, and stability, as well as with the ability to decrease the deposits of carbon on the catalyst during the DRM reaction. The coprecipitation method included the precipitant K_2CO_3. Subsequently, the impregnation of 1% of Co using cobalt acetylacetonat, was carried out for the preparation of $Co/Mg_{1-X}Ni_XO$ catalysts. Also, this research investigated the effects of the concentrations of CO_2 and CH_4 on the catalyst concentration and on the conversion temperature of the prepared catalysts in the DRM. Furthermore, this study attempted to evaluate the stability of the catalyst. This research study investigates the improvement in the conversion of methane for a stream of 1.25% O_2 gas passing through during the process.

2. Experimental

2.1 *Support and catalyst preparation*

In this work, we prepared catalysts of $Co/Mg_{1-x}Ni_xO$ (x= 0, 0.03, 0.07, 0.15; 1 wt% Co for each) through K_2CO_3 (Merck; >99.7%), co-precipitation from aqueous nickel nitrate hexahydrate and magnesium nitrate hexahydrate.[7] Following filtration and subsequent washing with warm water, the precipitate was dried for 12 h at 120 °C and pre-calcined at 500 °C in air for 5 h. The precipitate was pressed into disks at 600 kg/m^2 and calcined again at 1150 °C in air for 20 h. Afterwards, $Co/Ni_xMg_{1-x}O$ and Co/MgO catalysts were prepared by impregnating a support comprising of a $Co(C_5H_7O_2)_2 \cdot H_2O$ dichloromethane solution. After impregnation in the air for 12 h, the obtained catalysts were dried at 120 °C.

2.2 *Catalyst characterization*

The catalysts synthesized were characterized by XRD, FTIR, BET, and TEM, and XPS. X-ray diffraction analysis was performed using a Shimadzu diffractometer model XRD 6000. The diffractometer employed Cu-Kα radiation to generate diffraction patterns from powder crystalline samples at ambient temperature. The Cu-Kα radiation was generated by Philips glass diffraction X-ray tube broad focus 2.7 kW type. The crystallite size D of the samples was calculated using the Debye–Scherrer's relationship,[7] Where D is the crystalline size, λ is the incident X-ray wavelength, β is the full width at half-maximum (FWHM), and θ is the diffraction angle.

The Fourier transform infrared (FT-IR) analysis was carried out with PerkinElmer spectrometer model 100 series (sample preparation UATR). The total surface area of the catalysts was obtained using Brunauer-Emmett-Teller (BET) method with nitrogen adsorption at -196 °C. The analysis was conducted using a Thermo Fisher Scientific S.P.A (model: Surfer Analyzer) nitrogen adsorption-desorption analyzer. The Transmission Electron Microscopy (TEM, Model Hitachi H7100, Japan) was used to determine the crystal shape and Homogeneity of the Catalysts. Briefly, in deionized water, the powder was dispersed and dropped onto the Carbon-cover copper grids placed on a filter paper and at room temperature dried. XPS spectra were obtained using Kratos Axis Ultra DLD system, equipped with a mono-chromatic Al Kα (1486.6 eV), dual x-ray sources (Al & Mg), an argon etching system for sample cleaning and depth profiling, parallel imaging XPS, AES, ISS and Vision software for controlling the system. The base pressure of the analyzer chamber was 1×10^{-10} Torr. The excitation sources, X-ray gun was operated as a combination of 20 mA of emissions current and 15 kV voltages. The hemispherical analyzer was operated in the fixed analyzer transmission (FAT) mode for both wide and narrow scanning. This value is set at 100 eV and 40 eV of pass energy respectively. The region of interest for the narrow scan is corresponding to Mg2p, Ni2p, Co2p, and O1s photoelectron signal. The carbon charging correction refers to the binding energy of adventitious carbon at the binding energy of 285 eV. This highly sophisticated equipment is considered as a non-destructive analysis technique due to soft x-ray production to induce photoelectron emission from the sample surface. Therefore, the equipment would provide information about surface layers or thin film structures (about the top 10–100 Å of the sample).

2.3 *Catalyst evaluation*

Catalyst activity was evaluated for DRM in a continuous flow system by using a stainless-steel fixed-bed micro reactor (i.d. Ø = 6 mm, h = 34 cm), which was connected to the gas chromatography (GC) (Agilent 6890N; G 1540N) equipped with varian capillary columns HP-PLOT/Q and HP-MOLSIV and a mass-flow gas controller (SIERRA instrument). Before each reaction, about 0.02 g of catalyst was reduced by flowing 5% H_2/Ar at a rate of 30 mL/min from 200 °C to 700 °C held for 3 h. Methane reforming was carried out by flowing a gas mixture comprising 2:1 and 1:1 $CH_4:CO_2$ at a rate of 30 mL/min from 700 °C to 900 °C at atmospheric pressure held for 200 h.

3. Results and Discussion

3.1 *Characterization of the catalysts*

3.1a *XRD patterns*: Figure 1 shows XRD patterns for the related catalyst. The wide-angle XRD patterns of

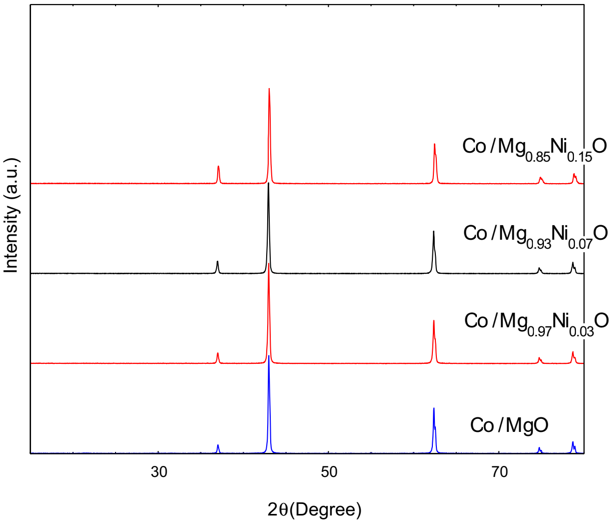

Figure 1. XRD patterns of the catalysts.

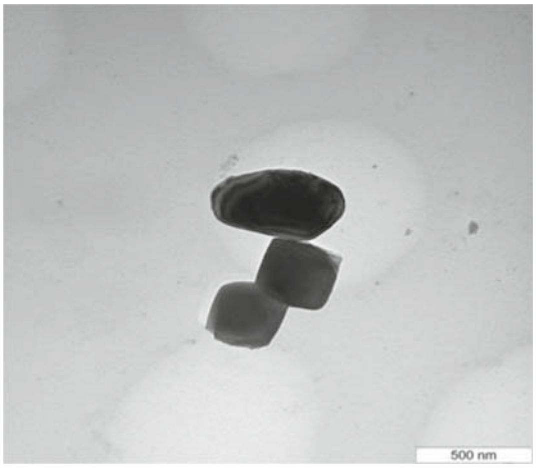

Figure 2. TEM image for $Co/Mg_{0.85}Ni_{0.15}O$.

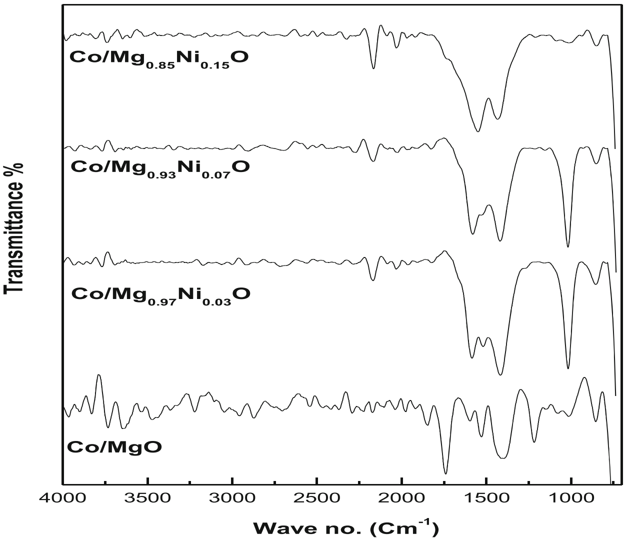

Figure 3. FTIR of catalyst.

NiO–MgO supported by cobalt catalysts revealed MgO reflections. Diffraction peaks were observed at about $2\theta = 39.7^\circ, 42.9^\circ, 62.5^\circ, 75^\circ$, and 79° and attributed to the cubic form of magnesia.[8] Diffraction lines were found at about $2\theta = 37^\circ, 43.1^\circ, 62.3^\circ, 74.8^\circ$, and 78.7°, and related to the cubic phase of nickel oxide. We also determined that the catalysts were in the cubic phase based on their crystal system, as indicated by the image of TEM as shown in Figure 2.

3.1b *FTIR & XPS*: Figure 3 shows the FTIR measurements. Ni-O, Co-O, and MgO bonds were present in the far-IR region, and all spectrum peaks were due to acetylacetonate. Figures 4a–d demonstrate photoelectron signals from Ni2p, C1s, Mg2p, and O1s as determined by the XPS data of the few top most nanometer layers on the catalyst surface. We identified three types of carbon species, namely, C-H (or C-C), C-O, and C=O, according to a deconvolution of a C1s narrow scan. Four oxygen species [O^{2-} (from the bulk), NiO, MgO, and CoO] contributed the O1s photoelectron signal.[8] This splitting was also attributed to the significant splitting of O1s spectrum, in which NiO had the highest photoelectron-signal intensity at the low-binding-energy region. We detected O^{2-}, NiO, CoO, and OH^- under a similar photoelectron envelope, but the contribution of OH^- was deemed to be very low at 533.0 eV binding energy. Furthermore, the oxide species of these metals were a mixture of MgO and $Mg(OH)_2$, NiO and $Ni(OH)_2$, and CoO as revealed by a narrow scan of Mg2p, Ni2p, and CoO, respectively.

Table 1 shows the values of BET specific surface area (S_{BET}) and the pore properties of catalyst supports and freshly prepared catalysts. The S_{BET} values decreased and the pore properties deteriorated in all three catalysts after impregnation, which may be due to pore blocking during impregnation.

Table 1 also presents the S_{BET} values, pore volumes, and average Co loadings of our prepared catalysts. Co/MgO and $Co/Mg_{0.97}Ni_{0.03}O$ had the largest pore volume and S_{BET} value,[9] respectively. No obvious relationship was found between the S_{BET} value and pore volume of catalysts, but the pore volume/S_{BET} ratio decreased in the order of Co/MgO, $Co/Mg_{0.97}Ni_{0.03}O$, $Co/Mg_{0.93}Ni_{0.07}O$, and $Co/Mg_{0.85}Ni_{0.15}O$. This result was consistent with the Co-dispersion order.

Aldoghachi *et al.*,[10] studied high pore volume/S_{BET} ratio and showed that it contributed to high catalyst performance. Table 1 shows the XRF results, in which Co loading was found to be $\leq 1\%$. This finding may be due to the loss of weight during support pre-calcination, thereby resulting in a high Ni content of catalysts.

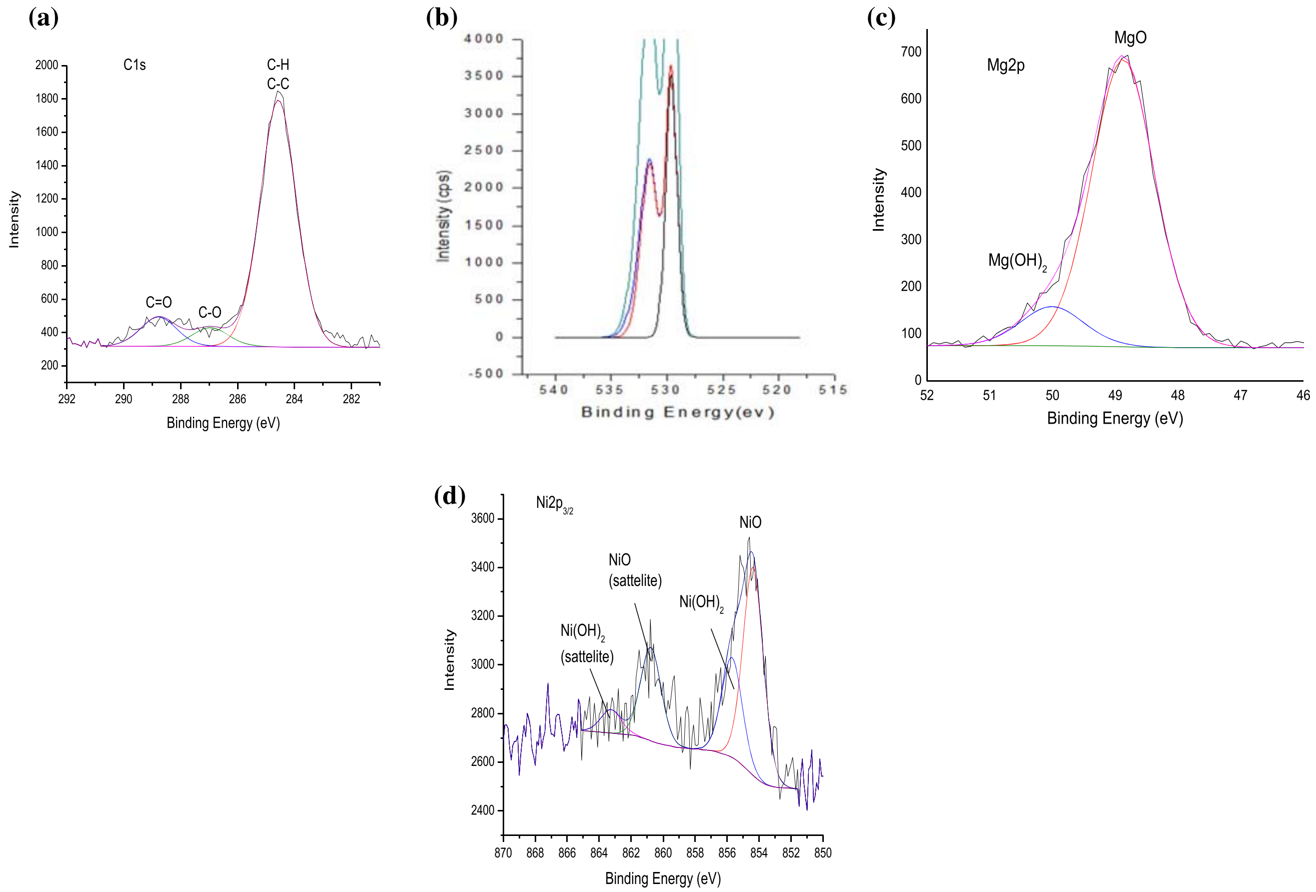

Figure 4. XPS of the Co/$Mg_{0.85}Ni_{0.15}O$ catalyst.

Table 1. The main textural properties of fresh catalysts.

Sample name	Specific surface area[a] m^2/g	Pore volume cm^3/g	Pore Volume to S_{BET} ratio 10^{-9} m	Pore radius Å	Co Loading[b] wt %	Average crystal size[c] nm
Co/MgO	8.23	0.41	40.6	19.34	0.94	43.0
Co/$Mg_{0.97}Ni_{0.03}O$	9.34	0.17	30.96	18.98	0.91	42.9
Co/$Mg_{0.93}Ni_{0.07}O$	10.11	0.06	31.9	19.44	0.90	42.6
Co/$Mg_{0.85}Ni_{0.15}O$	11.52	0.04	32.2	19.35	0.96	38.28

[a] Specific surface area calculated by BET method.
[b] Determined by the XRF method.
[c] Determined by the Debye-Scherrer equation of the Mg (200) plane of XRD.

3.2 *Catalytic performance in biogas reforming*

Catalyst activity in DRM was indicated by CH_4 and CO_2 conversion. H_2/CO ratio was used to express selectivity. The most active catalyst in DRM of biogas is shown in Figure 5. After the reaction proceeded for 200 h at 900 °C, the catalyst yielded 99% and 83% conversion for both CO_2 and CH_4, respectively, and the H_2/CO ratio was 1.2. CO_2 and CH_4 conversion decreased in the order of Co/$Mg_{0.85}Ni_{0.15}O$ > Co/$Mg_{0.93}Ni_{0.07}O$ > Co/$Mg_{0.97}Ni_{0.03}O$ > Co/MgO. Carbon formation may have had the highest resistance of deactivation, and thus the highest H_2 and CO selectivities were observed in 1:1 CH_4:CO_2 mole ratio.[10] BET results indicated that crucial to the conversion process were the pore size of supporter and doping metal. DRM of the biogas reaction was further performed in the presence of low-concentration oxygen (1.25%) flow and enhanced the conversion of CH_4 from 83 to 95%, results are shown in Figure 6. Initially, the reaction of this oxygen with

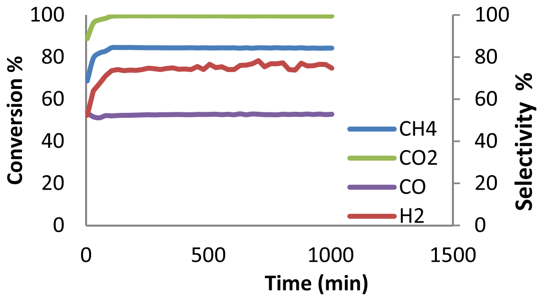

Figure 5. Stability tests of Co/$Mg_{0.85}Ni_{0.15}O$ fresh catalysts (a) and recycled catalysts at 900 °C for 200 h (GHSV = 15000 mL $cat^{-1}h^{-1}$, atmospheric pressure).

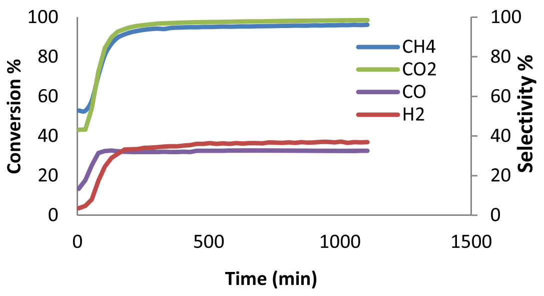

Figure 6. DRM reaction of the Co/$Mg_{0.85}$ $Ni_{0.15}O$ catalyst under 900 °C with 1.25% O_2.

methane to give CO and H_2O Eq. (4), thus, the syngas formed from their produced steam with the carbon deposition (Eq. (5)).

$$CH_4 + 1.5O_2 \rightarrow CO + 2H_2O \tag{4}$$

$$C(s) + H_2O \rightarrow CO + H_2 \tag{5}$$

Table 1 shows that with an increase in the concentration of NiO, there was an increase in the surface area from the BET result. The best result observed by the catalyst Co/ $Mg_{0.85}Ni_{0.15}O$ was found at the conversion rate of CH_4 and CO_2 as well as the ratio of H_2/CO. This phenomenon reveals that the incorporation of NiO into the MgO catalysts can significantly depress the Reverse Water Gas Shift (RWGS) reaction (Eq. 6).

$$CO_2 + H_2 \rightarrow CO + H_2O\,\Delta H^{\circ}_{298K} = 41.0\,\text{kJ/mol} \tag{6}$$

DRM reaction has been investigated and comparison of noble (Rh, Ru, Pd, Ir and Pt) and non-noble (Ni and Co) metal catalysts were made by Tsyganok *et al.*,[11] and reported that the Ni and Co catalysts showed higher catalytic activities compared to the noble metal-supported catalysts. However, the higher coke depositions of Ni and Co catalysts indicated their poor coke resistance ability compared to noble metal catalysts. Thus, the deactivation arising from the coke deposition is the major obstacle in the application of the Ni-based catalyst. As a result of this process the carbon deposition is reduced and consequently, the lifetime of the catalyst could be improved using Co/$Mg_{1-x}Ni_xO$ catalysts.

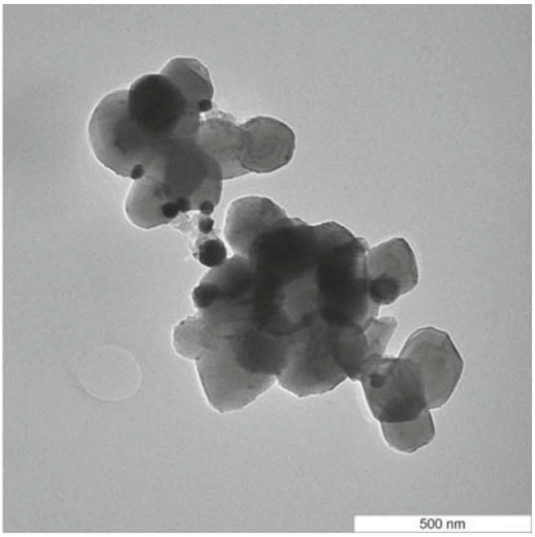

Figure 7. Co/$Mg_{0.85}Ni_{0.15}O$ after the 200 h reaction, at 900 °C, and CH_4/CO_2 ratio 1:1.

3.3 *Post-reaction characterization*

The image of TEM and TGA analysis detected the presence of a coke deposit with an oxygen stream of spent catalyst. Figure 7 illustrates the TEM images. The image shows that the original structure of the catalyst was maintained even after 200 h of stream testing. Furthermore, the spent catalyst kept its two-dimensional cubic texture. The phenomenon of a slight metal sintering was observed in the spent catalyst. Whilst the two-dimensional cubic channel of spent catalyst limited the sintering of the active metals inside the pore, the active metals supported on the outside surface experienced significant sintering. Since no filamentous carbon was found in the spent catalyst, it can be concluded that the coke deposition was negligible.

4. Conclusions

Dry reforming of methane over Co/$Mg_{1-x}Ni_xO$ catalysts was carried out for the production of syngas. The catalysts were synthesized using co-precipitation method and subsequently pre-screened by testing the catalytic performance in methane dry reforming reaction. The pre-screening test showed that Co/$Mg_{0.85}Ni_{0.15}O$ catalyst has the best catalytic performance in terms of conversion and yield. Hence, Co was selected as the active metal to be dispersed on the $Mg_{0.85}Ni_{0.15}O$ support. The interaction effects of factors such as concentration metals support, reactant (CH_4:CO_2) ratios (1:1 and 2:1) and reaction temperature (700 – 900 °C) were considered in the performance of the Co/$Mg_{0.85}Ni_{0.15}O$ in terms of CH_4 and CO_2 conversion as well as H_2 and CO yield. The Co/$Mg_{0.85}Ni_{0.15}O$ catalyst showed a promising performance at a reaction temperature of 900 °C and CH_4:CO_2 ratios at 1:1 with highest CH_4 and CO_2 conversions of 83% and 99% respectively. The Co/$Mg_{0.85}Ni_{0.15}O$ catalyst was subsequently characterized for its physicochemical properties by XRD, FTIR, TEM, EDX, BET and XPS. The methane dry reforming over the Co/$Mg_{0.85}Ni_{0.15}O$ gave syngas ratio of 1.2 making it suitable for the production of oxygenated fuel via Fischer-Tropsch synthesis. The reaction was further performed in the presence of low-concentration oxygen (1.25%) and enhanced the conversion of CH_4 from 83 to 95%.

Acknowledgements

This study was funded by the NanoMite Grant (Vot. No: 5526308).

References

1. Chin M J, Poh P E, Tey B T, Chan E S and Chin K L 2013 Biogas from palm oil mill effluent (POME): Opportunities and challenges from Malaysia's perspective *Renew. Sust. Energy Rev.* **26** 717
2. Poh P and Chong M 2009 Development of anaerobic digestion methods for palm oil mill effluent (POME) treatment *Bioresour. Technol.* **100** 1
3. Ashcroft A T, Cheetham A, Green M and Vernon P D 1991 Partial oxidation of methane to synthesis gas using carbon dioxide *Nature* **352** 225
4. Chen Q J, Zhang J, Jin Q W, Pan B R, Kong W B, Zhao T J and Sun Y H 2013 Effect of reflux digestion treatment on the catalytic performance of Ni-CaO-ZrO_2 nanocomposite catalysts for CO_2 reforming of CH_4 *Catal. Today* **215** 251
5. Ashok J and Kawi S 2013 Steam reforming of toluene as a biomass tar model compound over CeO_2 promoted Ni/CaO-Al_2O_3 catalytic systems *Int. J. Hydrogen Energy* **38** 13938
6. Liu Y, He Z, Zhou L, Hou Z and Eli W 2013 Simultaneous oxidative conversion and CO_2 reforming of methane to syngas over Ni/vermiculite catalysts *Catal. Commun.* **42** 40
7. Al-Doghachi F A, Rashid U and Taufiq-Yap Y H 2016 Investigation of Ce (III) promoter effects on the tri-metallic Pt, Pd, Ni/MgO catalyst in dry-reforming of methane *RSC Adv.* **6** 10372
8. Al-Doghachi F A, Islam A, Zainal Z, Saiman M I, Embong Z and Taufiq-Yap Y H 2016 High coke-resistance Pt/$Mg_{1-x}Ni_xO$ catalyst for dry reforming of methane *PLoS ONE* **11** e0145862
9. Saha B, Khan A, Ibrahim H and Idem R 2014 Evaluating the performance of non-precious metal based catalysts for sulfur-tolerance during the dry reforming of biogas *Fuel* **120** 202
10. Al-Doghachi F A, Rashid U, Zainal Z, Saiman M I and Taufiq-Yap Y H 2015 Influence of Ce_2O_3 and CeO_2 promoters on Pd/MgO catalysts in the dry-reforming of methane *RSC Adv.* **5** 81739
11. Tsyganok A I, Inaba M, Tsunoda T, Hamakawa S, Suzuki K and Hayakawa T 2003 Dry reforming of methane over supported noble metals: A novel approach to preparing catalysts *Catal. Commun.* **4** 493